

Federated Learning under Partially Disjoint Data via Manifold Reshaping

Anonymous authors

Paper under double-blind review

Abstract

Statistical heterogeneity severely limits the performance of federated learning (FL), motivating several explorations *e.g.*, FedProx, MOON and FedDyn, to alleviate this problem. Despite effectiveness, their considered scenario generally requires samples from almost all classes during the local training of each client, although some covariate shifts may exist among clients. In fact, the natural case of partially disjoint data (PDD), where each client contributes a few classes (instead of all classes) of samples, is practical yet underexplored. Specifically, the unique collapse and invasion characteristics of PDD can induce the biased optimization direction in local training, which prevents the efficiency of federated learning. To address this dilemma, we propose a manifold reshaping approach called FedMR to calibrate the feature space of local training. Our FedMR adds two interplaying losses to the vanilla federated learning: one is the intra-class loss to decorrelate feature dimensions for anti-collapse; and the other one is the inter-class loss to guarantee the proper margin among categories in the feature expansion. We conduct extensive experiments on a range of datasets to demonstrate that our FedMR achieves much higher accuracy and better communication efficiency.

1 Introduction

Federated learning McMahan et al. (2017); Li et al. (2020a); Yang et al. (2019) has drawn considerable attention due to the increasing requirements on data protection Shokri & Shmatikov (2015); Zhu & Han (2020); Hu et al. (2021); Li et al. (2021b); Lyu et al. (2020) in real-world applications like medical image analysis Guo et al. (2021); Park et al. (2021); Yin et al. (2022); Dou et al. (2021); Jiang et al. (2022) and autonomous driving Liang et al. (2019); Pokhrel & Choi (2020). Nevertheless, the resulting challenge of data heterogeneity severely limits the application of machine learning algorithms Zhao et al. (2018) in federated learning. This motivates a plenty of explorations to address the statistical heterogeneity issue and improve the efficiency Kairouz et al. (2021); Wang et al. (2020); Li et al. (2022).

Existing approaches to address the statistical heterogeneity can be roughly summarized into two categories. One line of research is to constrain the parameter update in local clients or in the central server. For example, FedProx Li et al. (2020b), FedDyn Acar et al. (2020) and FedDC Gao et al. (2022) explore how to reduce the variance or calibrate the optimization by adding the proximal regularization on parameters in FedAvg. The other line of research focuses on constraining the representation from the model to implicitly affect the update. FedProc Mu et al. (2021) and FedProto Tan et al. (2022) introduce prototype learning to help local training, and MOON Li et al. (2021a) utilizes contrastive learning to minimize the distance between representations learned by local model and global model, and maximize the distance between representations learned by local model and previous local model. However, all these methods validate their efficiency mostly under the support from all classes of samples in each client while lacking a well justification on a natural scenario, namely *partially disjoint data w.r.t. classes*.

As illustrated in Figure 1(a), in typical federated learning, each client usually contains all classes of samples but under different covariate shifts, and all clients work together to train a global model. However, in the case of PDD (Figure 1(b)), there are only a small subset of all categories in each client and all clients together provide information of all classes. Such a situation is actually very common in real-world applications. For example, there are shared and distinct Thyroid diseases in different hospitals due to regional diversity Gaitan et al. (1991). These hospitals from different regions can construct a federation to learn a comprehensive model for the diagnostic of Thyroid diseases but suffer from the PDD challenge. We conduct a toy study on a simulated dataset (see details in the Appendix B),

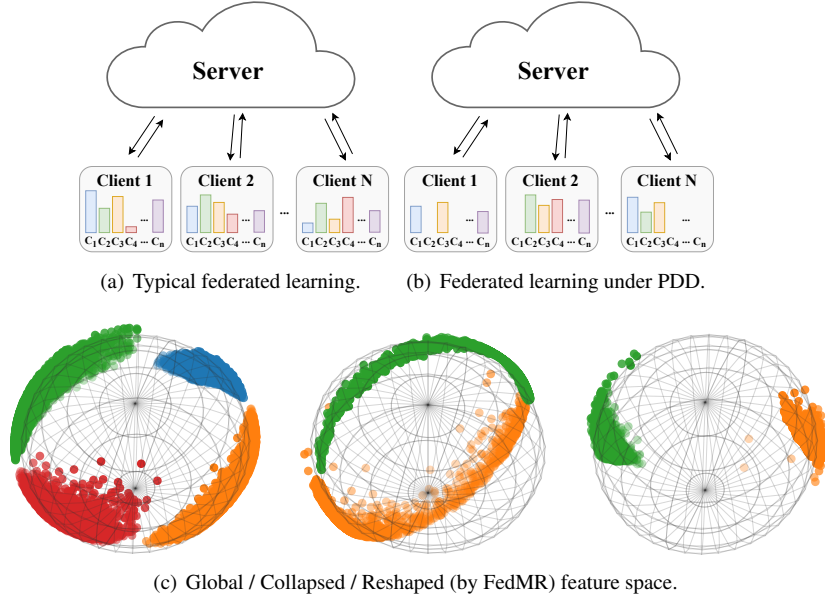


Figure 1: Federated learning under partially disjoint data (PDD).

and visualize the feature space under the centralized training (the left panel of Figure 1(c)) and that of local training under PDD (the middle panel of Figure 1(c)) by projecting on the unit sphere. From Figure 1(c), we can find that PDD induces a dimensional collapse onto a narrow area due to the lack of support from all classes, and causes a space invasion to the missing classes.

To our best knowledge, previous methods in federated learning have not formally explored the collapse and invasion characteristics of PDD, causing the algorithmic inefficiency in these scenarios. To address this dilemma, we propose a manifold-reshaping approach called FedMR to properly prevent the degeneration caused by the locally class missing. FedMR introduces two interplaying losses to the vanilla federated learning: one is intra-class loss to decorrelate feature space for the dimensional anti-collapse; and another one is the inter-class loss to guarantee the proper margin among categories by means of global class prototypes. The right panel of Figure 1(c) provides a rough visualization of FedMR. Theoretically, we analyze the benefit from the interaction of the intra-class loss and the inter-class loss under PDD, and empirically, we verify the effectiveness of FedMR compared with the current state-of-the-art methods. Our contributions can be summarized as follows:

- We are among the first attempts to study dimensional collapse and space invasion challenges caused by PDD in Generic FL that degenerates embedding space and thus limits the model performance.
- We introduce a principled approach termed as FedMR, which decorrelates the feature space to avoid dimensional collapse and constructs the proper inter-class margin to prevent space invasion. Our theoretical analysis confirms the rationality of the designed losses and their benefits to address the dilemma of PDD.
- We conduct a range of experiments on multiple benchmark datasets under the PDD case and a real-world disease dataset to demonstrate the advantages of FedMR over the state-of-the-art methods. We also develop several variants of FedMR to consider the communication cost and privacy concerns, and show their promise.

2 Related Works

2.1 Federated Learning

There are extensive works to address the *statistical heterogeneity* in federated learning, which induces the bias of local training due to the covariate shifts among clients Zhao et al. (2018); Li et al. (2022). A line of research handles

this problem by adding constraints like normalization or regularization on model weights in the local training or in the server aggregation. FedProx Li et al. (2020b) utilizes a proximal term to limit the local updates so as to reduce the bias, and FedNova Wang et al. (2020) introduces the normalization on total gradients to eliminate the objective inconsistency. FedDyn Acar et al. (2020) makes the global model and local models approximately aligned in the limit by proposing a dynamic regularizer for each client at each round. FedDC Gao et al. (2022) reduces the inconsistent optimization on the client-side by local drift decoupling and correction. Another line of research focuses on constraining representations from local models and the global model. MOON Li et al. (2021a) corrects gradients in local training by contrasting the representation from local model and that from global model. FedProc Mu et al. (2021) utilizes prototypes as global information to help correct local representations. Our FedMR is similarly conducted on representations of samples and classes but follows a totally different problem and spirit.

2.2 Representation Learning

The collapse problem is also an inevitable concern in the area of representation learning. In their research lines, there are several attempts to prevent the potential collapse issues. For example, in self-supervised learning, Barlow Twins, VICReg and Shuffled-DBN Bardes et al. (2022); Zbontar et al. (2021); Hua et al. (2021) manipulate the rank of the (co-)variance matrix to prevent the potential collapse. In contrastive learning, DirectCLR Jing et al. (2021) directly optimizes the representation space without an explicit trainable classifier to promote a larger feature diversity. In incremental learning, CwD Shi et al. (2022) applies a similar technique to prevent dimensional collapse in the initial phase. In our PDD case, it is more challenging, since we should not only avoid collapse but also avoid the space invasion in the feature space.

2.3 Federated Prototype Learning

In many vision tasks Snell et al. (2017); Yang et al. (2018); Deng et al. (2021), prototypes are the mean values of representations of a class and contain information like feature structures and relationships of different classes. Since prototypes are population-level statistics of features instead of raw features, which are relatively safe to share, prototype learning thus has been applied in federated learning. In Generic FL, FedProc Mu et al. (2021) utilizes the class prototypes as global knowledge to help correct local training. In Personalized FL, FedProtoTan et al. (2022) shares prototypes instead of local gradients to reduce communication costs. We also draw spirits from prototype learning to handle PDD. Besides, to make fair comparison to methods without prototypes and better reduce extreme privacy concerns, we conduct a range of auxiliary experiments in Section 4.4.

3 The Proposed Method

3.1 Preliminary

PDD Definition. There are many nonnegligible real-world PDD scenarios. ISIC2019 dataset Codella et al. (2018); Tschandl et al. (2018); Combalia et al. (2019), a region-driven *subset* of types of Thyroid diseases in the hospital systems, is utilized in our experiments. In landmark detection Weyand et al. (2020) for thousands of categories with data locally preserved, most contributors only have a *subset* of categories of landmark photos where they live or traveled before, which is also a scenario for the federated PDD problem. To make it clear, we first define some notations of the partially disjoint data situation in federated learning. Let C denote the collection of full classes and P denote the set of all local clients. Considering the real-world constraints like privacy or environmental limitation, each local client may only own the samples of partial classes. Thus, for the k -th client P_k , its corresponding local dataset D_k can be expressed as

$$D_k = \{(x_{k,i}, y_{k,i}) | y_{k,i} = c \in C_k\}, \text{ where } C_k \subsetneq C.$$

The number of samples of the class c ($c \in C_k$) in P_k is N_k^c . We denote a local model $f(\cdot; \mathbf{w}_k)$ on all clients as two parts: a backbone network $f_1(\cdot; \mathbf{w}_{k,1})$ and a linear classifier $f_2(\cdot; \mathbf{w}_{k,2})$. The loss of the k -th client can be formulated as

$$\ell_k^{\text{cls}}(D_k; w_k) = \frac{1}{N_k} \sum_{i=1}^{N_k} \ell(y_{k,i}, f_2(z_{k,i}; w_{k,2})) \Big|_{z_{k,i} = f_1(x_{k,i}; w_{k,1})},$$

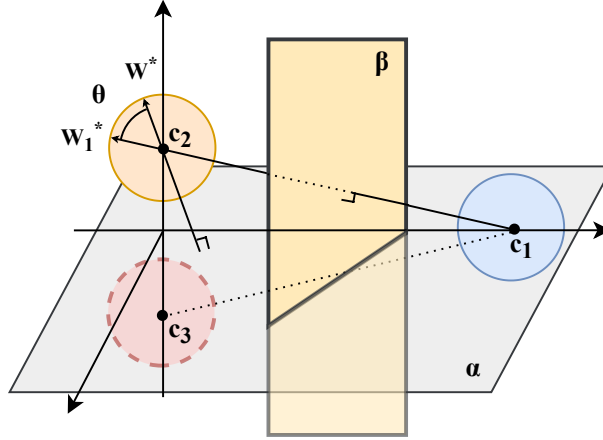


Figure 2: An illustration about the shift of the optimization direction under PDD. Here, we assume our client contains two classes c_1 and c_2 with one missing class c_3 . \mathbf{w}^* is the optimal classifier direction for c_2 (perpendicular to the plane α) when all classes exist, and \mathbf{w}_1^* is the learned classifier direction when c_3 is missing, which can be inferred by the decision plane β between c_1 and c_2 . As can be seen, PDD leads to the angle shift θ in the optimization.

where $z_{k,i}$ is the feature representation of the input $x_{k,i}$ and $\ell(\cdot, \cdot)$ is the loss measure like the cross-entropy function. Under PDD, we can empirically find the dimensional collapse and the space invasion problems about representation.

FedAvg. The vanilla federated learning via FedAvg consists of four steps McMahan et al. (2017): 1) In round t , the server distributes the global model \mathbf{w}^t to clients that participate in the training; 2) Each local client receives the model and continues to train the model, *e.g.*, the k -th client conducts the following,

$$\mathbf{w}_k^t \leftarrow \mathbf{w}_k^t - \eta \nabla \ell_k(b_k^t; \mathbf{w}_k^t), \quad (1)$$

where η is the learning rate, and b_k^t is a mini-batch of training data randomly sampled from the local dataset \mathcal{D}_k . After E epochs, we acquire a new local model \mathbf{w}_k^t ; 3) The updated models are then collected to the server as $\{\mathbf{w}_1^t, \mathbf{w}_2^t, \dots, \mathbf{w}_K^t\}$; 4) The server performs the following aggregation to acquire a new global model \mathbf{w}^{t+1} ,

$$\mathbf{w}^{t+1} \leftarrow \sum_{k=1}^K p_k \mathbf{w}_k^t, \quad (2)$$

where p_k is the proportion of sample number of the k -th client to the sample number of all the participants, *i.e.*, $p_k = N_k / \sum_{k'=1}^K N_{k'}$. When the pre-defined maximal round T reaches, we will have the final optimized model \mathbf{w}^T .

3.2 Motivation

In Figure 2, we illustrate a low-dimensional example to characterize the directional shift of the *local* training under PDD on the client side. In the following, we use the parameter aggregation of a linear classification to study the directional shift of *global* model in the server, which further clarifies the adverse effect of PDD. Similar to Figure 2, let c_1 , c_2 and c_3 denote three classes of samples respectively centered at $(1, 0)$, $(0, \sqrt{3})$ and $(0, -\sqrt{3})$ with radius $r = \frac{1}{2}$. Then, if there are samples of all classes in each local client, we will get the optimal weight for all categories as follows:

$$\mathbf{w}^* = \begin{bmatrix} 1 & 0 \\ -\frac{\sqrt{3}}{2} & \frac{1}{2} \\ -\frac{\sqrt{3}}{2} & -\frac{1}{2} \end{bmatrix}.$$

Note that, we omit the bias term in linear classification for simplicity. Conversely, among total three participants, if each participant only has the samples of two classes, *e.g.*, (c_1, c_2) , (c_1, c_3) and (c_2, c_3) respectively, then their learned

weights can be inferred as follows:

$$w_1^*, w_2^*, w_3^* = \begin{bmatrix} \frac{1}{2} & -\frac{\sqrt{3}}{2} \\ -\frac{1}{2} & \frac{\sqrt{3}}{2} \\ 0 & 0 \end{bmatrix}, \begin{bmatrix} \frac{1}{2} & \frac{\sqrt{3}}{2} \\ 0 & 0 \\ -\frac{1}{2} & -\frac{\sqrt{3}}{2} \end{bmatrix}, \begin{bmatrix} 0 & 0 \\ 0 & 1 \\ 0 & -1 \end{bmatrix}.$$

After the server aggregation, we have the estimated weight

$$\hat{w}^* = \begin{bmatrix} \frac{1}{3} & 0 \\ -\frac{1}{6} & \frac{\sqrt{3}+2}{6} \\ -\frac{1}{6} & -\frac{\sqrt{3}+2}{6} \end{bmatrix}.$$

Then, we can find that except the difference on amplitude between w^* and \hat{w}^* , a more important issue is the optimization direction for c_2 (or c_3) shifts about 45° by computing the angle between vector $(-\frac{\sqrt{3}}{2}, \frac{1}{2})$ and vector $(-\frac{1}{6}, \frac{\sqrt{3}+2}{6})$ (or between vector $(-\frac{\sqrt{3}}{2}, -\frac{1}{2})$ and vector $(-\frac{1}{6}, -\frac{\sqrt{3}+2}{6})$). Actually, the angle shift can be enlarged in some real-world applications, when the hard negative classes are missing.

3.3 Manifold Reshaping

As the aforementioned analysis, PDD in federated learning leads to the directional shift of optimization both in the local models and in the global model. An empirical explanation is that the feature representation of the specific class that should support classification is totally missing, inducing the feature representation of other observed classes arbitrarily distributes as a greedy collapsed manifold, as shown in Figure 1(c). To address this problem, we explore a manifold-reshaping method from both the intra-class perspective and the inter-class perspective. In the following, we will present two interplaying losses and our framework.

3.3.1 Intra-Class Loss

The general way to prevent the representation from collapsing into a low-dimensional manifold, *i.e.*, dimensional collapse, is to decorrelate dimensions for different patterns and expand the intrinsic dimensionality of each category. Such a goal can be implemented by manipulating the rank of the covariance matrix regarding representation. Specifically, for each client, we can first compute the class-level normalization for the representation $z_{k,i}^c$ as follows:

$$\hat{z}_{k,i}^c = \frac{z_{k,i}^c - \mu_k^c}{\sigma_k^c},$$

where μ_k^c and σ_k^c are the mean and standard deviation of features belonging to class c in the (mini-)batch. Then, we can compute an intra-class covariance matrix based on the above normalization for each observed class in the k -th client:

$$M_k^c = \frac{1}{N_k^c - 1} \sum_{i=1}^{N_k^c} \left(\hat{z}_{k,i}^c (\hat{z}_{k,i}^c)^\top \right),$$

With M_k^c , we can make its eigenvalues distributed uniformly to prevent the dimensional collapse of each observed class. However, considering the learnable pursuit of machine learning algorithms, we actually cannot directly optimize the eigenvalues to reach this goal. Fortunately, it is possible to use an equivalent objective as an alternative, which is clarified by the following lemma.

Lemma 1. *Assuming a covariance matrix $M \in \mathbf{R}^{d \times d}$ computed from the feature of each sample with the standard normalization, and its eigenvalues $\{\lambda_1, \lambda_2, \dots, \lambda_d\}$, we will have the following equality that satisfied*

$$\sum_{i=1}^d \left(\lambda_i - \frac{1}{d} \sum_{j=1}^d \lambda_j \right)^2 = \|M\|_F^2 - d.$$

The complete proof is summarized in the Appendix A.2. From Lemma 1, we can see that pursuing the uniformity of the eigenvalues for the covariance matrix can transform into minimizing the Frobenius norm of the covariance matrix. Therefore, our intra-class loss to prevent the undesired dimensional collapse for observed classes is formulated as

$$\ell_k^{\text{intra}} = \frac{1}{|C_k|} \sum_{c \in C_k} \|M_k^c\|_F^2. \quad (3)$$

3.3.2 Inter-Class Loss

Although the intra-class loss helps decorrelate the feature dimensions to prevent collapse, the resulting space invasion for the missing classes can be concomitantly exacerbated. Thus, it is important to guarantee the proper space of the missing classes in the expansion as encouraged by equation 3. To address this problem, we maintain a series of global class prototypes and transmit them to local clients as support of the missing classes in the feature space. Concretely, we first compute the class prototypes in the k -th client as follows:

$$\left\{ g_k^c \middle| g_k^c \leftarrow \frac{1}{N_k^c} \sum_{i=1}^{N_k^c} z_{k,i}^c \text{ for } c \in C_k \right\}.$$

Then, all client-level prototypes are submitted to the server along with local models in federated learning. In the central server, the global prototypes for all classes are updated as

$$\left\{ g_c^t \middle| g_c^t \leftarrow \sum_{k=1}^K p_k^c g_k^c \text{ for } c \in C \right\},$$

where g_c^t is the global prototype of the c -th class in round t and $p_k^c = N_k^c / \sum_{k=1}^K N_k^c$. In the next round, the central server distributes the global prototypes to all clients as the references to avoid the space invasion. Formally, we construct the following margin loss by contrasting the distances from prototypes to the representation of the sample.

$$\ell_k^{\text{inter}} = \frac{1}{|C_k|(|C_k| - 1)} \sum_{c_i \in C_k} \sum_{c_j \in C_k \setminus c_i} D_{c_i, c_j}, \quad (4)$$

where D_{c_i, c_j} is defined as:

$$D_{c_i, c_j} = \frac{1}{N_k^c} \sum_{n=1}^{N_k^c} \max\{\|z_{k,n}^{c_i} - g_{c_i}^t\| - \|z_{k,n}^{c_j} - g_{c_j}^t\|, 0\}.$$

In the following, we use a theorem to characterize how the inter-class loss jointly with the intra-class loss makes the representation of the missing classes approach to the optimal via the feature decorrelation and the prototype support.

Theorem 1. *Let the global optimal representation for class c denote by $g_c^* = [a_{c,1}^*, \dots, a_{c,d}^*]$, and $z_k^{c,t}$ denote the representation of sample x in the class c of the k -th client. Assuming that $\forall i$, both $|a_{c,i}^*|$ and $z_{k,i}^{c,t}$ are upper bounded by G , and all dimensions are disentangled. Then, in round t , the i -th dimension of local representation $z_{k,i}^{c,t}$ satisfies*

$$|z_{k,i}^{c,t} - a_{c,i}^*| \leq 2(1 - \hat{p}_k^c \Gamma)G + \delta \Gamma,$$

where \hat{p}_k^c is the accumulation regarding the i -th dimension of the class- c prototype, $\Gamma = \frac{1 - (p_k^c)^t}{1 - p_k^c}$ and δ is the maximum margin induced by the optimization of the inter-loss term.

Note that, Theorem 1 shows four critical points: 1) The proof of the theorem requires each dimension of the representation to be irrelevant to each other, which is achieved by the intra-class loss. 2) In the theorem, δ is a trade-off of training stability and theoretical results determined by the margin. The larger the margin, the larger the δ , however the more stable the local training is. This is because the global prototypes are not very accurate in the early stage of local training and directly minimizing the distance of samples to their global class prototypes can bring side effect to

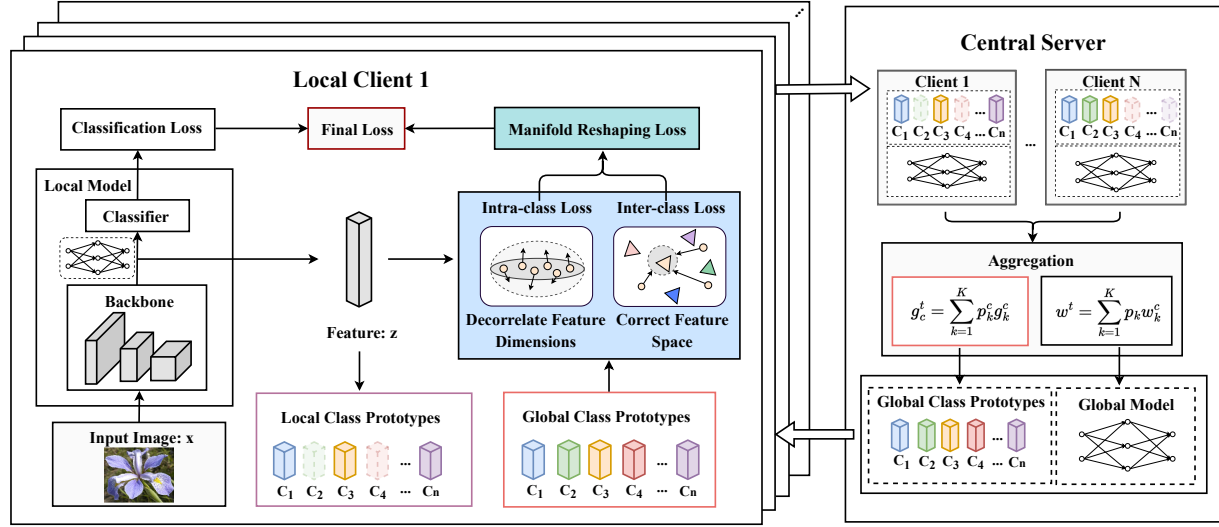


Figure 3: The framework of FedMR. On the client side, except the vanilla training with the classification loss, the manifold-reshaping parts, *i.e.*, the intra-class loss and the inter-class loss, respectively help conduct the feature decorrelation to avoid the dimensional collapse, and leverage the global prototypes to construct the proper margin among classes to prevent the space invasion. On the server side, except the model aggregation, the global class prototypes are also generated as the reference for missing classes participating in the local training.

Algorithm 1 FedMR

Input: a set of K clients that participate in each round, the initial model weights \mathbf{w}^0 , the maximal round T , the learning rate η , the local training epochs E .

for $t = 0, 1, \dots, T - 1$ **do**

▷ on the server side

randomly sample K clients

updates global model weights and global class prototypes ($\mathbf{w}^t \leftarrow \sum_{k=1}^K p_k^t \mathbf{w}_k^{t-1} \forall c, g_c^t \leftarrow \sum_{k=1}^K p_k^t g_k^c$).

distribute \mathbf{w}^t and $G_c\{g_1^t, g_2^t, \dots, g_C^t\}$ to the K clients.

▷ on the client side

do in parallel for $\forall k \in K$ **clients**

$\mathbf{w}_k^t \leftarrow \mathbf{w}^t$.

for $\tau = 0, 1, \dots, E - 1$ **do**

sample a mini-batch b_k^τ from local dataset and perform local updates ($\mathbf{w}_k^t \leftarrow \mathbf{w}_k^t - \eta \nabla \mathcal{L}_k(b_k^\tau, G_c; \mathbf{w}_k^t)$).

end for

update local class prototypes ($\forall c, g_k^c \leftarrow \sum_{i=1}^{n_k^c} \frac{1}{n_k^c} z_i^c$).

submit \mathbf{w}_k^t and $\{g_k^1, g_k^2, \dots, g_k^C\}$ to the server.

end in parallel

end for

the feature diversity. When the margin is removed ($D_{c_i, c_j} = \frac{1}{N_k^c} \sum_{n=1}^{N_k^c} \|z_{k,n}^{c_i} - g_{c_i}^t\|$), δ will be zero. 3) Without considering δ , as t increases, Γ is smaller and representation z_k^c is closer to global optimal prototype g_c^* , showing the promise of our method. 4) When t is large enough, we can get an upper bound $2 \frac{1-p_k^c - \hat{p}_k^c}{1-p_k^c} G$, meaning more clients with the specific dimensional information participating in the training, the tighter the upper bound is. When all other clients can provide the support ($\hat{p}_k^c = 1 - p_k^c$), the error will be 0. The complete proof is summarized in the Appendix A.1.

Table 1: Performance of FedMR and a range of state-of-the-art approaches on four datasets under PDD partitions. Datasets are divided into q clients and each client has ς classes (denoted as $PqC\varsigma$). We compute average accuracy of all partitions, highlight results of FedMR, underline results of best baseline, and show the improvement of FedMR to FedAvg (subscript of FedMR) and to the best baseline (Δ).

Datasets	Split	FedAvg	FedProx	FedProc	FedNova	MOON	FedDyn	FedDC	FedMR	Δ
FMNIST	P5C2	67.29	69.60	66.28	66.87	66.82	<u>71.01</u>	68.50	75.51 _{8.22%↑}	+4.50
	P10C2	67.33	67.76	<u>69.08</u>	48.44	67.93	67.16	67.36	74.97 _{7.64%↑}	+5.89
	P10C3	81.67	80.93	82.06	83.20	<u>83.42</u>	83.00	83.24	83.55 _{1.88%↑}	+0.13
	P10C5	88.53	89.22	<u>89.23</u>	88.86	88.98	88.38	89.22	90.04 _{1.51%↑}	+0.81
	IID	91.93	91.95	92.06	91.84	92.12	91.76	<u>92.15</u>	92.19 _{0.26%↑}	+0.04
	avg	79.35	79.89	79.74	75.84	79.87	<u>80.26</u>	80.09	83.45 _{4.10%↑}	+3.19
SVHN	P5C2	81.85	<u>81.83</u>	79.54	81.11	81.60	79.89	81.63	83.10 _{1.25%↑}	+1.27
	P10C2	78.92	79.60	78.75	66.86	<u>79.83</u>	76.24	78.96	82.47 _{3.55%↑}	+2.64
	P10C3	87.70	87.40	<u>88.13</u>	87.50	87.83	87.27	88.05	89.13 _{1.43%↑}	+1.00
	P10C5	91.20	91.24	91.63	<u>92.09</u>	91.16	90.17	91.64	92.18 _{0.98%↑}	+0.09
	IID	92.74	92.89	<u>93.57</u>	92.62	93.12	92.26	92.90	93.04 _{0.30%↑}	-0.53
	avg	86.48	86.59	86.32	83.87	<u>86.71</u>	85.17	86.64	87.98 _{1.50%↑}	+1.27
CIFAR10	P5C2	67.68	68.18	69.27	67.57	66.86	<u>69.64</u>	69.18	74.19 _{6.51%↑}	+4.55
	P10C2	67.27	<u>71.09</u>	67.02	57.79	67.61	67.74	67.64	73.32 _{2.23%↑}	+2.23
	P10C3	77.82	77.89	77.87	77.22	<u>78.42</u>	77.99	77.94	82.75 _{4.93%↑}	+4.33
	P10C5	88.22	88.34	88.19	88.20	88.00	<u>88.35</u>	88.14	89.06 _{0.84%↑}	+0.71
	IID	91.88	92.14	92.62	92.37	92.56	92.29	<u>92.85</u>	93.06 _{1.18%↑}	+0.21
	avg	78.58	<u>79.53</u>	78.99	76.63	78.69	79.20	79.15	82.48 _{3.90%↑}	+2.95
CIFAR100	P10C10	54.31	54.79	54.69	54.45	54.98	<u>55.94</u>	54.73	57.27 _{2.96%↑}	+1.33
	P10C20	64.81	65.37	64.98	<u>65.79</u>	65.75	65.02	65.21	65.81 _{1.00%↑}	+0.02
	P10C30	69.35	69.75	69.64	69.55	69.51	<u>69.84</u>	69.38	70.24 _{0.89%↑}	+0.40
	P10C50	71.28	71.35	<u>72.13</u>	71.25	71.54	71.25	72.11	72.17 _{0.89%↑}	+0.04
	IID	72.28	72.55	<u>73.07</u>	72.66	73.01	73.04	72.77	72.79 _{0.51%↑}	-0.28
	avg	66.41	66.76	66.90	66.74	66.96	<u>67.22</u>	66.84	67.66 _{1.25%↑}	+0.44

3.3.3 The Total Framework

After introducing the intra-class loss and the inter-class loss, we give the total framework of FedMR. On the client side, local models are trained on their partially disjoint datasets. Through manifold-reshaping loss, dimensions of the representation are decorrelated and local class subspace is corrected to prevent the space invasion, and gradually approach the global space partition. The total local objective including the vanilla classification loss can be written as

$$\mathcal{L}_k = \ell_k^{\text{cls}} + \underbrace{(\mu_1 \ell_k^{\text{intra}} + \mu_2 \ell_k^{\text{inter}})}_{\text{manifold reshaping}}, \quad (5)$$

where μ_1 and μ_2 are the balancing hyperparameters and will be discussed in the experimental part. In Figure 3, we illustrate the corresponding structure of FedMR and formulate the training procedure in Algorithm 1. In terms of the privacy concerns about the prototype transmission and the communication cost, we will give the comprehensive analysis on FedMR about these factors.

4 Experiment

4.1 Experimental Setup

Datasets. We adopt four popular benchmark datasets SVHN Netzer et al. (2011), FMNIST Xiao et al. (2017), CIFAR10 and CIFAR100 LeCun et al. (1998) in federated learning and a real-world PDD medical dataset

Table 2: Global test accuracy of methods on CIFAR10 and CIFAR100 under larger scale of clients (P10, P50 and P100) and ISIC2019. $P_{\varrho}C_{\varsigma}$ denotes that the dataset is divided into ϱ clients and each client has ς classes of samples. We highlight results of FedMR, underline results of best baseline, and show the improvement of FedMR to FedAvg (bottom right corner of results) and to the best baseline (Δ).

Datasets	Split	FedAvg	FedProx	FedProc	FedNova	MOON	FedDyn	FedDC	FedMR	Δ
CIFAR10	P10C3	77.82	77.89	77.87	77.22	<u>78.42</u>	77.99	77.94	82.75 _{4.93%↑}	+4.33
	P50C3	75.46	<u>77.46</u>	76.27	74.12	76.51	75.52	76.03	79.58 _{4.12%↑}	+2.12
	P100C3	71.65	<u>72.37</u>	72.44	70.46	72.46	71.85	<u>73.95</u>	76.93 _{5.28%↑}	+2.98
CIFAR100	P10C10	54.31	54.79	54.69	54.45	54.98	55.94	54.73	57.27 _{2.96%↑}	+1.33
	P50C10	49.84	51.17	51.94	50.22	<u>52.19</u>	50.53	51.17	53.36 _{3.52%↑}	+1.17
	P100C10	47.90	48.26	49.01	48.07	48.94	<u>49.24</u>	48.76	49.60 _{1.70%↑}	+0.36
ISIC2019	Real	73.14	75.41	75.26	73.62	<u>75.46</u>	75.07	75.25	76.55 _{3.41%↑}	+1.09

ISIC2019 Codella et al. (2018); Tschandl et al. (2018); Combalia et al. (2019) to conduct experiments. Regarding the data setup, although Dirichlet Distribution is popular to split data in federated learning, it usually generates diverse imbalance data coupled with occasionally PDD. In order to better study pure PDD, for the former four benchmarks, we split each dataset into ϱ clients, each with ς categories, abbreviated as $P_{\varrho}C_{\varsigma}$. For example, P10C10 in CIFAR100 means that we split CIFAR100 into 10 clients, each with 10 classes. Please refer to the detailed explanations and strategies in the Appendix. ISIC2019 is a real-world federated application under the PDD situation and the data distribution among clients is shown in the Appendix C.1.3. We follow the settings in Flamby benchmark Terrail et al. (2022).

Implementation. We compare FedMR with FedAvg McMahan et al. (2017) and multiple state-of-the-arts including FedProx Li et al. (2020b), FedProc Karimireddy et al. (2020), FedNova Li et al. (2021a), MOON Wang et al. (2020), FedDyn Acar et al. (2020) and FedDC Gao et al. (2022). To make a fair and comprehensive comparison, we utilize the same model for all approaches and three model structures for different datasets: ResNet18 He et al. (2016) (follow Li et al. (2021a; 2022)) for SVHN, FMNIST and CIFAR10, wide ResNet Zagoruyko & Komodakis (2016) for CIFAR100 and EfficientNet Tan & Le (2019) for ISIC2019. The optimizer is SGD with a learning rate 0.01, the weight decay 10^{-5} and momentum 0.9. The batch size is set to 128 and the local updates are set to 10 epochs for all approaches. The detailed information of the model and training parameters are given in the Appendix.

4.2 Performance under PDD

In this part, we compare FedMR with FedAvg and other methods on FMNIST, SVHN, CIFAR10 and CIFAR100 datasets under partially disjoint situation. Note that, in FedProx, MOON, FedDyn, FedProc, FedDC and our method, there are parameters that need to set. Here we use grid search to choose the best parameters for each method. The concrete parameters and communications rounds are shown in the Appendix C.2. All other settings follow Section 4.1.

As shown in Table 1, with the decreasing class number in local clients, the performance of FedAvg and all other methods greatly drops. However, comparing with all approaches, our method FedMR achieves far better improvement to FedAvg, especially 7.64% improvement vs. 1.75% of FedProc for FMNIST (P10C2) and 6.51% improvement vs. 1.96% of FedDyn for CIFAR10 (P5C2). Besides, FedMR also performs better in less PDD situation, and on average of all partitions listed in the table, our method outperforms the best baseline by 3.19% on FMNIST and 2.95% on CIFAR10.

4.3 Scalability and Robustness

In the previous section, we validate the FedMR under 5 or 10 local clients under partially disjoint data situations. In order to make a comprehensive comparison, we increase the client numbers of CIFAR10 and CIFAR100 and in each round, only 10 of clients participate in the federated procedures. Besides, we also add one real federated application

Table 3: The communication cost of approaches with prototypes (*i.e.*, FedProc and FedMR) and without prototypes (*i.e.*, FedAvg, FedProx, FedNova, MOON, FedDyn and FedDC).

Method Type	FMNIST	SVHN	CIFAR10	CIFAR100	ISIC2019
w/o Prototypes	11.182M	11.184M	11.184M	36.565M	4.875M
w/ Prototypes	11.187M	11.189M	11.189M	36.629M	4.880M
Additional cost	0.044% \uparrow	0.044% \uparrow	0.044% \uparrow	0.175% \uparrow	0.102% \uparrow

Table 4: Number of communication rounds and the speedup of communication when reaching the best accuracy of FedAvg in federated learning on CIFAR100 under three partition strategies.

Method (CIFAR100)	P10C10		P50C10		P100C10	
	Commu.	Speedup	Commu.	Speedup	Commu.	Speedup
FedAvg	400	1 \times	400	1 \times	400	1 \times
FedProx	352	1.14 \times	370	1.08 \times	384	1.04 \times
FedProc	357	1.12 \times	381	1.05 \times	389	1.03 \times
FedNova	290	1.38 \times	385	1.04 \times	<u>382</u>	<u>1.05</u> \times
MOON	332	1.20 \times	373	1.07 \times	395	1.01 \times
FedDyn	<u>178</u>	<u>2.25</u> \times	<u>366</u>	<u>1.09</u> \times	384	1.04 \times
FedDC	275	1.45 \times	393	1.02 \times	387	1.03 \times
FedMR	149	2.68 \times	293	1.37 \times	368	1.09 \times

ISIC2019 with multiple statistical heterogeneity problems including PDD. The exact parameters and communication rounds of all methods can be found in the Appendix C.2.

In Table 2, we divide CIFAR10 and CIFAR100 into 10, 50 and 100 clients and keep the PDD degree in the same level. As can be seen, with the number of client increasing, the performance of all methods drops greatly. No matter in the situations of fewer or more clients, our method achieves better performance and outperforms best baseline by 2.98% in CIFAR-10 and 0.95% in CIFAR-100 on average. Besides, in Table 2, we also verify FedMR with other methods under a real federated applications: ISIC2019. As shown in the last line of Table 2, our method achieves the best improvement of 3.41% relative to FedAvg and of 1.09% relative to best baseline MOON, which means our method is robust in more complicated situations more than PDD.

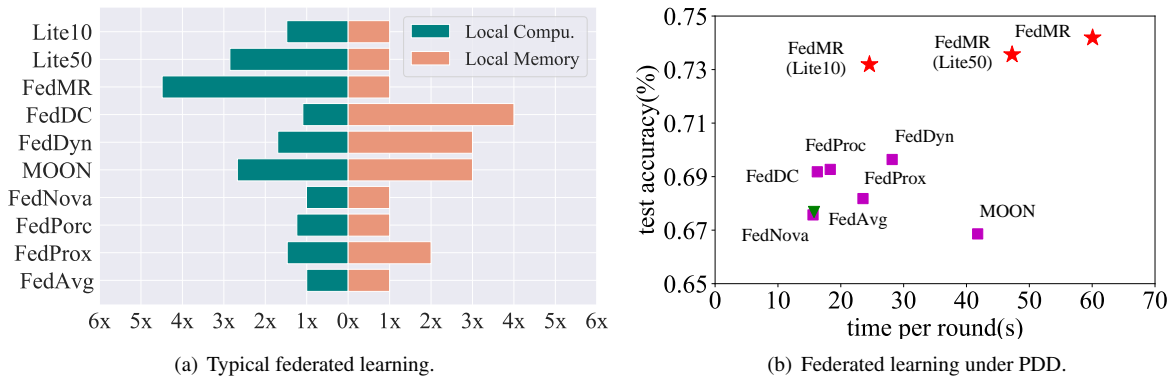


Figure 4: The average memory consuming and computation time of local training on all datasets of all baselines, FedMR and its light versions (Lite 10 and Lite 50) for accelerating.

Table 5: Performance of FedMR on CIFAR10 and CIFAR100 when only 50%, 80% and 100% of clients are allowed to submit their class prototypes under different partitions. $P_{\varrho C \varsigma}$ means that the dataset is divided into ϱ clients and each client has ς classes.

Datasets	Split	FedAvg	50%	80%	100%
CIFAR10	P10C3	77.82	80.42	80.27	82.75
	P50C3	75.46	79.14	79.43	79.58
	P100C3	71.65	76.73	76.87	76.93
CIFAR100	P10C10	54.31	56.41	56.73	57.27
	P50C10	50.22	51.06	52.57	53.36
	P100C10	47.90	48.80	48.88	49.60

Table 6: The ablation study of FedMR. We illustrate average accuracy of FedMR on FMNIST, SVHN, CIFAR10 and CIFAR100 without the inter-class loss or the intra-class loss or both. Results of all partitions of four datasets are shown in Appendix C.4.

Inter	Intra	FMNIST	SVHN	CIFAR10	CIFAR100
-	-	79.35	86.48	78.58	66.41
✓	-	80.18	87.46	78.86	66.62
-	✓	81.03	87.15	80.89	67.11
✓	✓	83.45	87.98	82.48	67.66

4.4 Further Analysis

Except performance under PDD, we here discuss the communication cost between clients and server, local burden of clients, and privacy, and conduct the ablation study.

Communication Concern. In terms of communication cost, our method needs to share the additional prototypes. To show how much extra communication cost will be incurred, in Table 3, we show the number of transmission parameters in each round to compare the communication cost of methods with prototypes (FedProc and FedMR) and without prototypes (FedAvg, FedProx, FedNova, MOON, FedDyn and FedDC). From the results, the additional communication cost in single round is negligible. In Table 4, we also provide the communication rounds on CIFAR100 under three different partitions, where all methods require to reach the best accuracy of FedAvg within 400 rounds. From the table 4, we can see that FedMR uses less communication rounds (best speedup) to reach the given accuracy, indicating that FedMR is a communication-efficient approach.

Local Burden Concern. In real-world federated applications, local clients might be mobile phones or other small devices. Thus, the burden of local training can be the bottleneck for clients. In Figure 4(a), we compute the number of parameters that needs to be saved in local clients and the average local computation time in each round. As can be seen, FedDC, FedDyn and MOON require triple or even quadruple storing memory than FedAvg, while FedProc and FedMR only need little space to additionally store prototypes. In terms of local computation time, FedMR requires more time to carefully reshape the feature space. To handle some computing-restricted clients, we provide light versions of FedMR, namely Lite 10 and Lite 50, where local clients randomly select only 10 or 50 samples to compute inter-class loss. From Figure 4(a), the training time of Lite 10 and Lite 50 decreases sharply, while their performance is still competitive and better than other baselines, as shown in Figure 4(b). Please refer to Appendix C.3 for more details.

Privacy Concern. Although prototypes are population-level statistics of features instead of raw features, which are relatively safe Mu et al. (2021); Tan et al. (2022), it might be still hard for some clients with extreme privacy limitations. To deal with this case, one possible compromise is allowing partial local clients not to submit prototypes. In Table 5, we verify this idea for FedMR on CIFAR10 and CIFAR100, where at the beginning, we only randomly

Table 7: Variance of top 50 eigenvalues of covariance matrices of all classes within a mini-batch on CIFAR10.

Method	P5C2	P10C2	P10C3	P10C5	IID
FedAvg	1201	1274	1055	814	640
FedMR (intra)	478	437	372	407	538
FedMR (inter+intra)	570	538	566	579	635

Table 8: The average accuracy of all methods adopted in Table 1 with or without the aid of prototypes on FMNIST. Since FedProc is the prototype version of FedAvg, here we don’t show them.

Method	FedProx	FedNova	MOON	FedDyn	FedDC	FedMR
w/o Prototypes	79.89	75.84	79.87	<u>80.26</u>	80.09	81.03
w Prototypes	80.29	78.76	80.12	<u>81.21</u>	80.57	83.45

pre-select 50% and 80% clients to require prototypes. From Table 5, even under the prototypes of 50% clients, FedMR still performs better than FedAvg, showing the elastic potential of FedMR in the privacy-restricted scenarios. In the extreme case where all prototypes of clients are disallowed to be submitted, we can remove the inter-class that depends on prototypes from FedMR and use the vanilla federated learning with the intra-class loss. As shown in Table 6, it can achieve a promising improvement than that without the intra-class loss. Note that, we cannot counteract the privacy concerns of federated learning itself, and leave this in the future explorations.

Decorrelating Analysis Here, we empirically verify the effectiveness of the intra-class loss on decorrelating the feature dimensions. In Table 7, we show the variance of top-50 eigenvalues (sort from the largest to the smallest) of the covariance matrix M within a mini-batch (batchsize is 128) after training 100 rounds on CIFAR10, namely,

$$\frac{1}{128} \sum_{i=1}^{50} (\lambda_i - \frac{1}{50} \sum_{j=1}^{50} \lambda_j)^2.$$

As can be seen, when the PDD problem eased, the variance of FedAvg gradually drops, which means in more uniform data distribution, the variance should be relatively small. The sharp decreasing variance indicates that the intra-class loss successfully decorrelates the dimensions. However the variance under the intra-class loss is too small and far away from the values of FedAvg in the IID setting, meaning it may enlarge the risk of the space invasion. In order to prevent space invasion, our inter-class loss provide a margin for the feature space expansion. In the table, we could see that the variance of FedMR (under the intra-class loss and the inter-class loss) is a little larger compared to FedMR (the intra-class loss) and approaches to the FedAvg under the IID setting.

Ablation Study. FedMR introduces two interplaying losses, the intra-class loss and the inter-class loss, to vanilla FL. To verify the individual efficiency, we conduct an ablation experiment in Table 6. As can be seen, the intra-class loss generally plays a more important role in the performance improvement of FedMR, but their combination complements each other and thus performs best than any of the single loss, confirming our intuition to prevent the collapse and space invasion under PDD jointly. Besides, as FedMR and FedProc need local clients additionally share class prototypes which might not fair for other baselines, in Table 8, we properly configure all baselines with prototypes on FMNIST to show the superiority of FedMR.

5 Conclusion

In this work, we study the problem of *partially disjoint data* (PDD) in federated learning, which is practical and challenging due to the unique collapse and invasion problems, and propose a novel approach called FedMR to address the dilemma of PDD. Theoretically, we show how the proposed two interplaying losses in FedMR to prevent the collapse and guarantee the proper margin among classes. Extensive experiments show that FedMR achieves significant improvements on FedAvg under the PDD situations and outperforms a range of state-of-the-art methods.

References

- Durmus Alp Emre Acar, Yue Zhao, Ramon Matas, Matthew Mattina, Paul Whatmough, and Venkatesh Saligrama. Federated learning based on dynamic regularization. In *International Conference on Learning Representations*, 2020.
- Adrien Bardes, Jean Ponce, and Yann Lecun. Vicreg: Variance-invariance-covariance regularization for self-supervised learning. In *ICLR 2022-10th International Conference on Learning Representations*, 2022.
- Noel CF Codella, David Gutman, M Emre Celebi, Brian Helba, Michael A Marchetti, Stephen W Dusza, Aadi Kallou, Konstantinos Liopyris, Nabin Mishra, Harald Kittler, et al. Skin lesion analysis toward melanoma detection: A challenge at the 2017 international symposium on biomedical imaging (isbi), hosted by the international skin imaging collaboration (isic). In *2018 IEEE 15th international symposium on biomedical imaging (ISBI 2018)*, pp. 168–172. IEEE, 2018.
- Marc Combalia, Noel CF Codella, Veronica Rotemberg, Brian Helba, Veronica Vilaplana, Ofer Reiter, Cristina Carrera, Alicia Barreiro, Allan C Halpern, Susana Puig, et al. Bcn20000: Dermoscopic lesions in the wild. *arXiv preprint arXiv:1908.02288*, 2019.
- Jiankang Deng, Jia Guo, Jing Yang, Alexandros Lattas, and Stefanos Zafeiriou. Variational prototype learning for deep face recognition. In *Proceedings of the IEEE/CVF Conference on Computer Vision and Pattern Recognition*, pp. 11906–11915, 2021.
- Qi Dou, Tiffany Y So, Meirui Jiang, Quande Liu, Varut Vardhanabhuti, Georgios Kaissis, Zeju Li, Weixin Si, Heather HC Lee, Kevin Yu, et al. Federated deep learning for detecting covid-19 lung abnormalities in ct: a privacy-preserving multinational validation study. *NPJ digital medicine*, 4(1):1–11, 2021.
- Eduardo Gaitan, Norman C Nelson, and Galen V Poole. Endemic goiter and endemic thyroid disorders. *World journal of surgery*, 15(2):205–215, 1991.
- Liang Gao, Huazhu Fu, Li Li, Yingwen Chen, Ming Xu, and Cheng-Zhong Xu. Feddc: Federated learning with non-iid data via local drift decoupling and correction. In *Proceedings of the IEEE/CVF Conference on Computer Vision and Pattern Recognition*, pp. 10112–10121, 2022.
- Pengfei Guo, Puyang Wang, Jinyuan Zhou, Shanshan Jiang, and Vishal M Patel. Multi-institutional collaborations for improving deep learning-based magnetic resonance image reconstruction using federated learning. In *Proceedings of the IEEE/CVF Conference on Computer Vision and Pattern Recognition*, pp. 2423–2432, 2021.
- Kaiming He, Xiangyu Zhang, Shaoqing Ren, and Jian Sun. Deep residual learning for image recognition. In *Proceedings of the IEEE conference on computer vision and pattern recognition*, pp. 770–778, 2016.
- Rui Hu, Yanmin Gong, and Yuanxiong Guo. Federated learning with sparsification-amplified privacy and adaptive optimization. In *IJCAI*, 2021.
- Tianyu Hua, Wenxiao Wang, Zihui Xue, Sucheng Ren, Yue Wang, and Hang Zhao. On feature decorrelation in self-supervised learning. In *Proceedings of the IEEE/CVF International Conference on Computer Vision*, pp. 9598–9608, 2021.
- Meirui Jiang, Zirui Wang, and Qi Dou. Harmofl: Harmonizing local and global drifts in federated learning on heterogeneous medical images. In *Proceedings of the AAAI Conference on Artificial Intelligence*, volume 36, pp. 1087–1095, 2022.
- Li Jing, Pascal Vincent, Yann LeCun, and Yuandong Tian. Understanding dimensional collapse in contrastive self-supervised learning. In *International Conference on Learning Representations*, 2021.
- Peter Kairouz, H Brendan McMahan, Brendan Avent, Aurélien Bellet, Mehdi Bennis, Arjun Nitin Bhagoji, Kallista Bonawitz, Zachary Charles, Graham Cormode, Rachel Cummings, et al. Advances and open problems in federated learning. *Foundations and Trends® in Machine Learning*, 14(1–2):1–210, 2021.

- Sai Praneeth Karimireddy, Satyen Kale, Mehryar Mohri, Sashank Reddi, Sebastian Stich, and Ananda Theertha Suresh. Scaffold: Stochastic controlled averaging for federated learning. In *International Conference on Machine Learning*, pp. 5132–5143. PMLR, 2020.
- Yann LeCun, Léon Bottou, Yoshua Bengio, and Patrick Haffner. Gradient-based learning applied to document recognition. *Proceedings of the IEEE*, 86(11):2278–2324, 1998.
- Qinbin Li, Bingsheng He, and Dawn Song. Model-contrastive federated learning. In *Proceedings of the IEEE/CVF Conference on Computer Vision and Pattern Recognition*, pp. 10713–10722, 2021a.
- Qinbin Li, Zeyi Wen, Zhaomin Wu, Sixu Hu, Naibo Wang, Yuan Li, Xu Liu, and Bingsheng He. A survey on federated learning systems: vision, hype and reality for data privacy and protection. *IEEE Transactions on Knowledge and Data Engineering*, 2021b.
- Qinbin Li, Yiqun Diao, Quan Chen, and Bingsheng He. Federated learning on non-iid data silos: An experimental study. In *2022 IEEE 38th International Conference on Data Engineering (ICDE)*, pp. 965–978. IEEE, 2022.
- Tian Li, Anit Kumar Sahu, Ameet Talwalkar, and Virginia Smith. Federated learning: Challenges, methods, and future directions. *IEEE Signal Processing Magazine*, 37(3):50–60, 2020a.
- Tian Li, Anit Kumar Sahu, Manzil Zaheer, Maziar Sanjabi, Ameet Talwalkar, and Virginia Smith. Federated optimization in heterogeneous networks. *Proceedings of Machine Learning and Systems*, 2:429–450, 2020b.
- Xinle Liang, Yang Liu, Tianjian Chen, Ming Liu, and Qiang Yang. Federated transfer reinforcement learning for autonomous driving. *arXiv preprint arXiv:1910.06001*, 2019.
- Lingjuan Lyu, Han Yu, and Qiang Yang. Threats to federated learning: A survey. *arXiv preprint arXiv:2003.02133*, 2020.
- Brendan McMahan, Eider Moore, Daniel Ramage, Seth Hampson, and Blaise Aguera y Arcas. Communication-efficient learning of deep networks from decentralized data. In *Artificial intelligence and statistics*, pp. 1273–1282. PMLR, 2017.
- Xutong Mu, Yulong Shen, Ke Cheng, Xueli Geng, Jiaxuan Fu, Tao Zhang, and Zhiwei Zhang. Fedproc: Prototypical contrastive federated learning on non-iid data. *arXiv preprint arXiv:2109.12273*, 2021.
- Yuval Netzer, Tao Wang, Adam Coates, Alessandro Bissacco, Bo Wu, and Andrew Y Ng. Reading digits in natural images with unsupervised feature learning. *NIPS Workshop on Deep Learning and Unsupervised Feature Learning*, 2011.
- Sangjoon Park, Gwanghyun Kim, Jeongsol Kim, Boah Kim, and Jong Chul Ye. Federated split task-agnostic vision transformer for covid-19 cxr diagnosis. *Advances in Neural Information Processing Systems*, 34, 2021.
- Shiva Raj Pokhrel and Jinho Choi. Federated learning with blockchain for autonomous vehicles: Analysis and design challenges. *IEEE Transactions on Communications*, 68(8):4734–4746, 2020.
- Yujun Shi, Kuangqi Zhou, Jian Liang, Zihang Jiang, Jiashi Feng, Philip HS Torr, Song Bai, and Vincent YF Tan. Mimicking the oracle: An initial phase decorrelation approach for class incremental learning. In *Proceedings of the IEEE/CVF Conference on Computer Vision and Pattern Recognition*, pp. 16722–16731, 2022.
- Reza Shokri and Vitaly Shmatikov. Privacy-preserving deep learning. In *Proceedings of the 22nd ACM SIGSAC conference on computer and communications security*, pp. 1310–1321, 2015.
- Jake Snell, Kevin Swersky, and Richard Zemel. Prototypical networks for few-shot learning. *Advances in neural information processing systems*, 30, 2017.
- Mingxing Tan and Quoc Le. Efficientnet: Rethinking model scaling for convolutional neural networks. In *International conference on machine learning*, pp. 6105–6114. PMLR, 2019.

- Yue Tan, Guodong Long, Lu Liu, Tianyi Zhou, Qinghua Lu, Jing Jiang, and Chengqi Zhang. Fedproto: Federated prototype learning across heterogeneous clients. In *AAAI Conference on Artificial Intelligence*, volume 1, pp. 3, 2022.
- Jean Ogier du Terrail, Samy-Safwan Ayed, Edwige Cyffers, Felix Grimberg, Chaoyang He, Regis Loeb, Paul Mangold, Tanguy Marchand, Othmane Marfoq, Erum Mushtaq, et al. Flamby: Datasets and benchmarks for cross-silo federated learning in realistic healthcare settings. *arXiv preprint arXiv:2210.04620*, 2022.
- Philipp Tschandl, Cliff Rosendahl, and Harald Kittler. The ham10000 dataset, a large collection of multi-source dermatoscopic images of common pigmented skin lesions. *Scientific data*, 5(1):1–9, 2018.
- Jianyu Wang, Qinghua Liu, Hao Liang, Gauri Joshi, and H Vincent Poor. Tackling the objective inconsistency problem in heterogeneous federated optimization. *arXiv preprint arXiv:2007.07481*, 2020.
- Tobias Weyand, Andre Araujo, Bingyi Cao, and Jack Sim. Google landmarks dataset v2-a large-scale benchmark for instance-level recognition and retrieval. In *Proceedings of the IEEE/CVF conference on computer vision and pattern recognition*, pp. 2575–2584, 2020.
- Han Xiao, Kashif Rasul, and Roland Vollgraf. Fashion-mnist: a novel image dataset for benchmarking machine learning algorithms. *arXiv preprint arXiv:1708.07747*, 2017.
- Hong-Ming Yang, Xu-Yao Zhang, Fei Yin, and Cheng-Lin Liu. Robust classification with convolutional prototype learning. In *Proceedings of the IEEE conference on computer vision and pattern recognition*, pp. 3474–3482, 2018.
- Qiang Yang, Yang Liu, Tianjian Chen, and Yongxin Tong. Federated machine learning: Concept and applications. *ACM Transactions on Intelligent Systems and Technology (TIST)*, 10(2):1–19, 2019.
- Youtan Yin, Hongzheng Yang, Quande Liu, Meirui Jiang, Cheng Chen, Qi Dou, and Pheng-Ann Heng. Efficient federated tumor segmentation via normalized tensor aggregation and client pruning. In *International MICCAI Brainlesion Workshop*, pp. 433–443. Springer, 2022.
- Sergey Zagoruyko and Nikos Komodakis. Wide residual networks. In *British Machine Vision Conference 2016*. British Machine Vision Association, 2016.
- Jure Zbontar, Li Jing, Ishan Misra, Yann LeCun, and Stéphane Deny. Barlow twins: Self-supervised learning via redundancy reduction. In *International Conference on Machine Learning*, pp. 12310–12320. PMLR, 2021.
- Yue Zhao, Meng Li, Liangzhen Lai, Naveen Suda, Damon Civin, and Vikas Chandra. Federated learning with non-iid data. *arXiv preprint arXiv:1806.00582*, 2018.
- Ligeng Zhu and Song Han. Deep leakage from gradients. In *Federated learning*, pp. 17–31. Springer, 2020.